https://doi.org/10.15407/ujpe67.9.645

V.A. NESTEROV, O.I. DAVYDOVSKA, V.YU. DENISOV

Institute for Nuclear Research, Nat. Acad. of Sci. of Ukraine
(47 Nauky Ave., Kyiv 03028, Ukraine; e-mail: v.nest.v@gmail.com)

ELASTIC SCATTERING CROSS-SECTIONS OBTAINED ON THE BASIS OF THE POTENTIAL OF THE MODIFIED THOMAS–FERMI METHOD AND TAKING THE CORE INTO ACCOUNT

Nucleon density distributions and nucleus-nucleus interaction potentials for the reactions $^{16}O + {}^{40}Ca$, $^{16}O + {}^{56}Fe$, and $^{16}O + {}^{90}Zr$ have been calculated in the framework of the modified Thomas–Fermi method and considering all terms up to the second order in $\hbar$ in the quasi-classical expansion of the kinetic energy. Skyrme forces dependent on the nucleon density are used as the nucleon-nucleon interaction. A parametrization of the nucleus-nucleus interaction potential, which well describes the potential value calculated within the modified Thomas–Fermi approach with density-dependent Skyrme forces, is found. On the basis of the obtained potentials, the cross-sections of elastic scattering are calculated in a good agreement with experimental data.

K e y w o r d s: nucleus-nucleus interaction potential, modified Thomas–Fermi method, nucleon density distribution, cross-section, repulsive core, elastic scattering.

1. Introduction

One of the main tasks of theoretical nuclear physics during the whole period of its existence has been the study of the peculiarities of the interaction between atomic nuclei. To calculate such fundamental parameters of nuclear reactions as the cross-sections of various processes, it is necessary, first of all, to know the potential energy of nuclear interaction [1–4]. From this point of view, of particular interest is the information on the magnitude and radial dependence of the interaction potential at short distances between nuclei.

Unfortunately, the potential of nucleon-nucleon interaction, especially of its nuclear component, has not been determined with a required accuracy till now. In general, it can be said that the potential can be qualitatively divided into the nuclear, Coulomb, and centrifugal components. The properties of the last two have already been studied rather well. But the situation with the nuclear part is much more complicated. A large number of various models are used now for its approximation [1–25]. However, the barrier heights in the corresponding potentials of nucleus-nucleus interaction, which affect the mechanism of nuclear reactions, can differ substantially among those models. For this reason, the information about the nucleus-nucleus interaction potential and the barrier height is principally important for describing the reaction process.

For this work, among all the methods used to construct the nucleus-nucleus interaction potential [26–36], we chose the semimicroscopic approach. In this approach, the nucleon and energy density distributions are calculated using the modified Thomas–Fermi method with density-dependent Skyrme forces [4, 7, 8, 10, 11, 13–25]. For now, there are a lot of successful Skyrme interaction parametrizations. In the presented work, we used the SkM* parametrization [32]. In this case, the semiclassical series expansion of the kinetic energy in Planck's constant $\hbar$ includes all possible terms up to $\hbar^2$. Previous calculations performed by us and other authors for specific nuclear problems testified that this is a rather accurate approximation, which will also be used in the future. Under such conditions, the modified Thomas–Fermi approach with Skyrme forces describes well the nucleon density distribution, the binding energy, the mean square radii, and many other characteristics of the ground and excited states of atomic nuclei [26–32, 34].

In the modified Thomas–Fermi approximation with Skyrme forces, the nucleus-nucleus potential approaches the Coulomb one at long distances. At small distances between the surfaces of colliding nuclei, a potential barrier is observed, which is associated with the Coulomb repulsion of the nuclei and with their nuclear attraction. As the distance between the nuclei diminishes further, the potential energy gradually decreases. However, in the modified Thomas–Fermi approximation with Skyrme forces, the nucleus-nucleus potential has a repulsive core at rather short distances between the nuclei, when the volumes of the colliding nuclei significantly overlap each other [7, 10, 13, 14, 17–22]. This repulsive core is associated with the considerable incompressibility of nuclear matter [13, 14, 19, 22].

Note that the repulsion at small distances between the nuclei exists in the proximity potential [5] and in the microscopic approach [37, 38]. Elastic scattering of light nuclei making allowance for the potential core was studied in works [13, 14, 19, 22, 39–41]. The account for the repulsive component of the potential made it possible to describe the deep subbarrier hindrance of the fusion of heavy nuclei [42–44]. However, the nucleus-nucleus potentials with a repulsive core are very rarely used to describe the scattering parameters of nuclei. Therefore, the study of the elastic scattering of heavy nuclei in the framework of the modified Thomas–Fermi approach with Skyrme forces and with regard for the core is an important and challenging task.

In Sections 2 and 3, we present mathematical methods that are necessary for the implementation of the chosen approach. Sections 4 and 5 contain a discussion of the obtained results and our conclusions, respectively.

2. Calculation of the Potential in the Framework of the Modified Thomas–Fermi Method

As was already indicated, the nucleus-nucleus interaction potential $V(R)$ consists of the nuclear, $V_N(R)$, Coulomb, $V_{\rm COUL}(R)$, and centrifugal, $V_l(R)$, components, which depend on the distance R between the centers of mass of the nuclei,

$$V(R) = V_N(R) + V_{\rm COUL}(R) + V_l(R). \tag{1}$$

For the Coulomb and centrifugal components, we used well-known expressions that can be found, in particular, in works [20, 23, 24].

Let us calculate the nuclear component $V_N(R)$ of the interaction potential in the framework of the extended Thomas–Fermi method and consider all terms up to the second order in $\hbar$ in the semiclassical expansion of the kinetic energy [4, 7, 8, 10, 11, 13–25]. As the nucleon-nucleon interaction, the density-dependent Skyrme forces, namely the SkM* parametrization [32], will be used. In our calculations, we deal with the approximation of "frozen" densities, which is quite applicable at the near-barrier energies.

The nucleus-nucleus interaction potential is defined as the difference between the energies of a system of two nuclei located at a finite distance, $E_{12}(R)$, and the infinite one, $E_{1(2)}$, from each other [8, 10],

$$V(R) = E_{12}(R) - (E_1 + E_2), \tag{2}$$

where

$$E_{12} = \int \epsilon\left[\rho_{1p}(\mathbf{r}) + \rho_{2p}(\mathbf{r}, R), \rho_{1n}(\mathbf{r}) + \rho_{2n}(\mathbf{r}, R)\right] d\mathbf{r}, \tag{3}$$

$$E_{1(2)} = \int \epsilon\left[\rho_{1(2)p}(\mathbf{r}), \rho_{1(2)n}(\mathbf{r})\right] d\mathbf{r}. \tag{4}$$

$\rho_{1(2)n}$ and $\rho_{1(2)p}$ are the neutron, n, and proton, p, densities of nuclei 1 and 2; $\epsilon\left[\rho_{1(2)p}(\mathbf{r}), \rho_{1(2)n}(\mathbf{r})\right]$ is the energy density; and R is the distance between the centers of mass of the nuclei. Note that the energy of the system at the infinite distance between the nuclei, $E_1 + E_2$, is the sum of the binding energies for separate nuclei.

The energy density in the integrand consists of the kinetic and potential components. If the Skyrme forces are used, its form is well known [24–28, 30, 32, 44]:

$$\begin{aligned}
\epsilon &= \frac{\hbar^2}{2m}\tau + \epsilon_{\rm Skyrme} + \epsilon_{\rm C} = \\
&= \frac{\hbar^2}{2m}\tau + \frac{1}{2}t_0\left[\left(1+\frac{1}{2}x_0\right)\rho^2 - \left(x_0+\frac{1}{2}\right)(\rho_n^2+\rho_p^2)\right] + \\
&+ \frac{1}{12}t_3\rho^\alpha\left[\left(1+\frac{1}{2}x_3\right)\rho^2 - \left(x_3+\frac{1}{2}\right)(\rho_n^2+\rho_p^2)\right] + \\
&+ \frac{1}{4}\left[t_1\left(1+\frac{1}{2}x_1\right) + t_2\left(1+\frac{1}{2}x_2\right)\right]\tau\rho + \\
&+ \frac{1}{4}\left[t_2\left(x_2+\frac{1}{2}\right) - t_1\left(x_1+\frac{1}{2}\right)\right](\tau_n\rho_n + \tau_p\rho_p) +
\end{aligned}$$

$$+\frac{1}{16}\left[3t_1\left(1+\frac{1}{2}x_1\right)-t_2\left(1+\frac{1}{2}x_2\right)\right](\nabla\rho)^2 \quad (5)$$

$$-\frac{1}{16}\left[3t_1\left(x_1+\frac{1}{2}\right)+t_2\left(x_2+\frac{1}{2}\right)\right]((\nabla\rho_p)^2+(\nabla\rho_n)^2)+$$

$$+\frac{1}{2}W_0[J\nabla\rho+J_n\nabla\rho_n+J_p\nabla\rho_p]+\epsilon_{\mathrm{C}}. \quad (6)$$

Here, τ is the kinetic energy density (its expression will be given below); m is the nucleon mass; t_0, t_1, t_2, t_3, x_0, x_1, x_2, x_3, α, and W_0 are the Skyrme interaction parameters; and ϵ_C is the Coulomb field energy density with regard for the direct and exchange terms in the Slater approximation [4, 7, 10, 27]. The terms proportional to t_0 and t_3 correspond to zero-range forces. The term proportional to t_0 is associated with attraction, whereas the term with t_3 corresponds to repulsion and increases, as the density of nuclear matter grows, which prevents the collapse of nuclear systems. The summands proportional to t_1 and t_2 make a correction for the finite range of action of nuclear forces. As the nucleon density increases, the contribution of those terms to the total energy increases as well. The constants x_0, x_1, x_2, and x_3 describe exchange effects; they are associated with the spin and isospin asymmetries. The parameter W_0 is the spin-orbit interaction constant.

With an accuracy to the second order in $\hbar$, the kinetic energy density has the form $\tau = \tau_{\mathrm{TF}} + \tau_2$ [7, 8, 10, 11, 24, 27, 28, 44], where, in turn, $\tau = \tau_n + \tau_p$ is the sum of the kinetic energy densities for protons and neutrons. We can write (see, e.g., works [27, 28]),

$$\tau_{\mathrm{TF},n(p)} = k\rho_{n(p)}^{5/3} \quad (7)$$

is the kinetic energy density of neutrons (protons) in the Thomas–Fermi approximation, $k = \frac{5}{3}(3\pi^2)^{2/3}$, and τ_2 is the complete expression for the second-order (in $\hbar$) gradient correction [27, 28],

$$\tau_{2n(p)} = b_1\frac{(\nabla\rho_{n(p)})^2}{\rho_{n(p)}} + b_2\nabla^2\rho_{n(p)} +$$

$$+ b_3\frac{\nabla f_{n(p)}\nabla\rho_{n(p)}}{f_{n(p)}} + b_4\rho_{n(p)}\frac{\nabla^2 f_{n(p)}}{f_{n(p)}} +$$

$$+ b_5\rho_{n(p)}\frac{(\nabla f_{n(p)})^2}{f_{n(p)}^2} + b_6h_m^2\rho_{n(p)}\left(\frac{\mathbf{W}_{n(p)}}{\rho_{n(p)}}\right)^2. \quad (8)$$

In formula (8), $b_1 = 1/36$, $b_2 = 1/3$, $b_3 = 1/6$, $b_4 = 1/6$, $b_5 = -1/12$, and $b_6 = 1/2$ are numerical coefficients; $h_m = \hbar^2/2m$; and the last term accounts for the spin-orbit interaction. The notation $\mathbf{W}_{n(p)}$ in formula (8) stands for

$$\mathbf{W}_{n(p)} = \frac{\delta\varepsilon(r)}{\delta\mathbf{J}_{n(p)(r)}} = \frac{W_0}{2}\nabla(\rho+\rho_{n(p)}), \quad (9)$$

and the quantity

$$f_{n(p)} = 1 + \frac{2m}{\hbar^2}\left[\frac{1}{4}\left[t_1\left(1+\frac{x_1}{2}\right)+t_2\left(1+\frac{x_2}{2}\right)\right]\rho + \right.$$

$$\left. + \frac{1}{4}\left[t_2\left(x_2+\frac{1}{2}\right)-t_1\left(x_1+\frac{1}{2}\right)\right]\rho_{n(p)}\right], \quad (10)$$

is expressed via the parameters of Skyrme forces x_1, x_2, t_1, t_2, and W_0, which depend on the parametrization choice. The contribution of the Thomas–Fermi term is dominant, especially in the nuclear bulk; but, at the nuclear surface, the gradient corrections begin to play a substantial role.

In this work, we consider the elastic scattering reactions ^{16}O + ^{40}Ca, ^{16}O + ^{56}Fe, and ^{16}O + ^{90}Zr. Let us calculate the nucleus-nucleus interaction potential for those systems in the framework of the modified Thomas–Fermi approach. For this purpose, it is necessary to know the densities of nucleon distributions in the interacting nuclei. We will use the nucleon densities obtained in the framework of the same modified Thomas–Fermi approach with Skyrme forces. For Skyrme forces, we will use the SkM* parametrization [32]. The nucleon distribution densities calculated for the ^{16}O, ^{40}Ca, ^{90}Zr, and ^{56}Fe nuclei in the framework of this method are shown in Fig. 1.

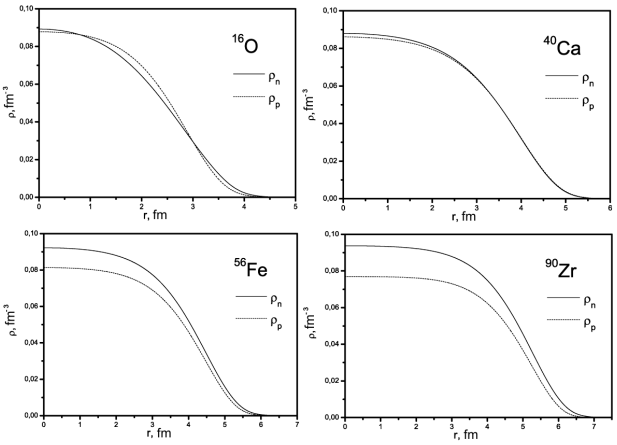

Fig. 1. Nucleon distribution densities for the ^{16}O, ^{40}Ca, ^{56}Fe, and ^{90}Zr nuclei obtained in the framework of the modified Thomas–Fermi method

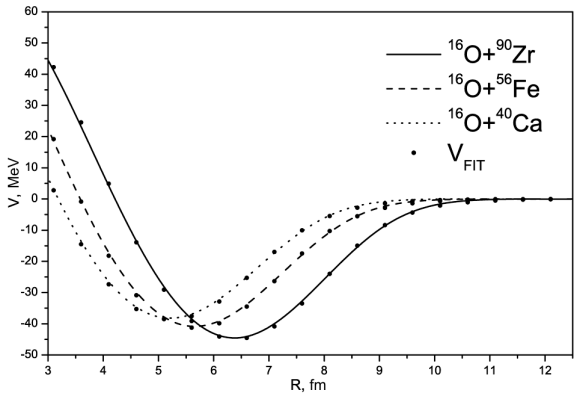

Fig. 2. Interaction potentials for the reactions ^{16}O + ^{40}Ca, ^{16}O + ^{90}Zr, and ^{16}O + ^{56}Fe obtained in the framework of the modified Thomas–Fermi method with the corresponding potential $V_{\rm FIT}$ taken in the analytic form (14)

Now, knowing the nucleon densities, we can obtain an expression for the energy density and calculate the nucleus-nucleus interaction potential in the framework of the modified Thomas–Fermi approach with Skyrme forces [formulas (1)–(10)]. In Fig. 2, the nuclear parts of the interaction potentials obtained for the reactions ^{16}O + ^{40}Ca, ^{16}O + ^{56}Fe, and ^{16}O + ^{90}Zr are shown. The obtained potentials look quite realistic and demonstrate a substantial repulsive core at short distances.

3. Analytic Expression for the Interaction Potential

For the convenience of further calculations, let us express the obtained potential in such a way that enables one to work with it in an analytic form. In so doing, for an adequate description of the elastic scattering cross-sections, it is very important to account for the repulsive core, which imposes certain requirements on the form of potential parametrization. From this viewpoint, the traditional form of Woods–Saxon parametrization does not suit us. For our analytic potential to possess a more realistic form, let us add another term to it. The expression for this term is similar to that for the kinetic energy in the Thomas–Fermi method, which should provide the necessary repulsion at short distances. We do this operation in a certain analogy with what was done in work [20], where we operated with double convolution potentials, which substantially improved the results obtained in this way. Therefore, the general expression for the potential takes the form

$$V_{\rm FIT}(R) = V_{\rm WS}(R) + V_{\rm kin}(R), \tag{11}$$

where $V_{\rm WS}(R)$ is the well-known Woods–Saxon potential

$$V_{\rm WS}(R) = \frac{-V_0}{1+e^{\frac{(R-R_0)}{d_0}}}, \tag{12}$$

and $V_{\rm kin}(R)$ is the kinetic term. In the Thomas–Fermi method, the kinetic energy is proportional to $\rho^{5/3}$ [see Eq. (7)], so the kinetic term is approximated using the well-known Fermi distribution for the density,

$$V_{\rm kin}(R) = \left(\frac{V_c}{1+e^{\frac{(R-C)}{a}}}\right)^{5/3}. \tag{13}$$

Table 1. **Parameters of the analytic representation of the potential for the considered reactions**

Reaction	V_0, MeV	R_0, fm	d_0, fm	V_c, MeV$^{3/5}$	C, fm	a, fm
^{16}O + ^{40}Ca	49.094	6.683	0.686	20.603	3.175	1.081
^{16}O + ^{90}Zr	54.2604	7.960	0.673	19.339	4.491	0.995
^{16}O + ^{56}Fe	51.9102	7.155	0.685	20.460	3.662	1.066

Table 2. **Parameters of the imaginary part of potential (15) for the ^{16}O + ^{40}Ca, ^{16}O + ^{90}Zr, and ^{16}O + ^{56}Fe reactions**

$E_{\rm lab}$, MeV	W_W, MeV	r_W, fm	d_W, fm	W_S, MeV	r_S, fm	d_S, fm
^{16}O + ^{40}Ca						
40	20.331	1.195	0.449	10.998	1.267	0.500
47	20.876	1.199	0.434	11.999	1.229	0.500
60	21.901	1.123	0.300	12.000	1.269	0.632
^{16}O + ^{90}Zr						
50	20.149	1.100	0.303	6.858	1.298	0.521
80	20.170	1.109	0.300	11.938	1.299	0.646
138.2	21.471	1.100	0.319	13.601	1.299	0.770
^{16}O + ^{56}Fe						
38	19.460	1.123	0.300	5.006	1.229	0.778
40	20.756	1.162	0.304	5.184	1.187	0.799
42	21.179	1.199	0.302	5.578	1.299	0.573
44	22.373	1.100	0.313	6.615	1.299	0.566
50	24.532	1.267	0.300	8.295	1.153	0.899
54	25.647	1.211	0.300	8.500	1.271	0.551
58	25.786	1.147	0.300	8.520	1.284	0.576

As a result, our analytic potential acquires the following final form:

$$V_{\rm FIT}(R) = \frac{-V_0}{1+e^{\frac{(R-R_0)}{d_0}}} + \left(\frac{V_c}{1+e^{\frac{(R-C)}{a}}}\right)^{5/3}. \qquad (14)$$

Formula (14) contains six fitting parameters: V_0, R_0, d_0, V_c, C, and a. Their values are determined by minimizing the most accurate realistic potential found in the framework of the modified Thomas–Fermi approach with Skyrme forces. The resulting values of the potential parameters for the reactions considered in this work are quoted in Table 1.

Figure 2 demonstrates the approximations of the nuclear part of the interaction potentials using expression (14), which were calculated for the interacting heavy nuclei in the reactions ^{16}O + ^{40}Ca, ^{16}O + ^{56}Fe and ^{16}O + ^{90}Zr in the framework of the modified Thomas–Fermi approach with Skyrme forces. The approximation turned out so accurate that the deviations are practically invisible on the plot scale. Thus, the proposed form of the fitting potential can very well describe the realistic nucleus-nucleus interaction potential obtained by numerical calculations.

4. Calculations of Elastic Scattering Cross-Sections

Making use of the determined nucleus-nucleus interaction potentials (14) with the relevant parameters (see Table 1) as the real part, let us calculate the elastic scattering cross-sections in the framework of the optical model. The imaginary part of the potential is taken in the form [2, 4]

$$W(R) = -\frac{W_W}{1+\exp[R-r_W(A_1^{1/3}+A_2^{1/3})/d_W]} - \\ - \frac{W_S\ \exp[R-r_S(A_1^{1/3}+A_2^{1/3})/d_S]}{d_S\ (1+\exp[R-r_W(A_1^{1/3}+A_2^{1/3})/d_W])^2}, \qquad (15)$$

where W_W, r_W, d_W, W_S, r_S, and d_S are the strength, radius, and diffusivity of the bulk (W) and surface (S) parts of the imaginary nuclear potential. This form for the imaginary part of the potential is widely used while describing various nuclear reactions. We consider elastic scattering reactions for the ^{16}O + ^{40}Ca system at the beam energies $E_{\rm lab} = 40$, 47, and 60 MeV; for the ^{16}O + ^{90}Zr system at the beam energies $E_{\rm lab} = 50$, 80, and 138.2 MeV; and for the

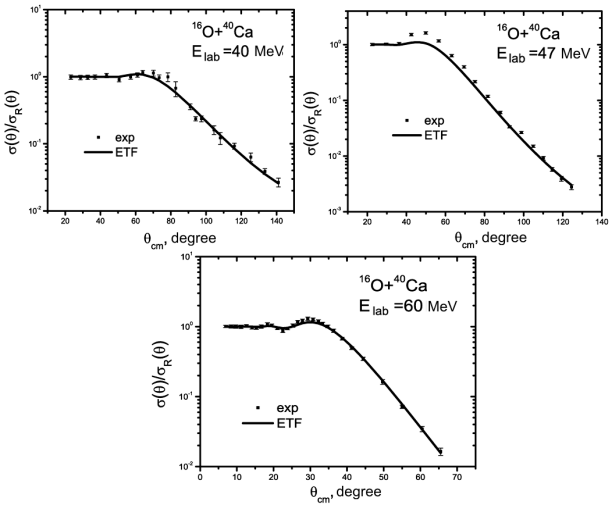

Fig. 3. Elastic scattering cross-sections for the ^{16}O + ^{40}Ca system at the beam energies $E_{\rm lab} = 40$, 47, and 60 MeV calculated in the modified Thomas–Fermi approximation with density-dependent Skyrme forces (ETF). Experimental data (exp) were taken from works [45, 46]

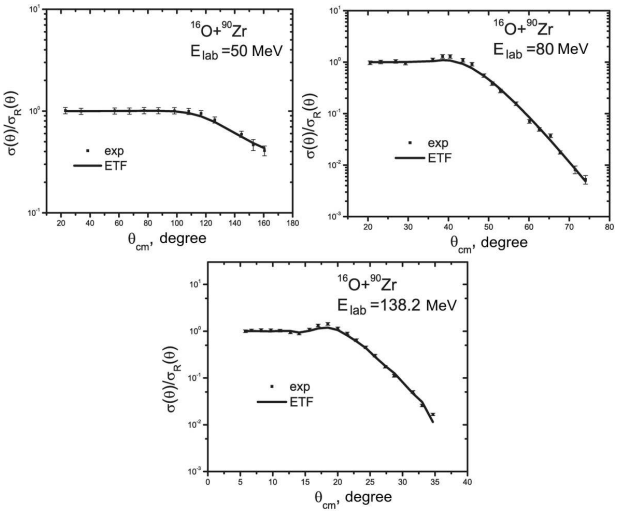

Fig. 4. Elastic scattering cross-sections for the ^{16}O + ^{90}Zr system at the beam energies $E_{\rm lab} = 50$, 80, and 138.2 MeV calculated in the modified Thomas–Fermi approximation with density-dependent Skyrme forces (ETF). Experimental data (exp) were taken from work [47]

^{16}O + ^{56}Fe system at the beam energies $E_{\rm lab} = 38$, 40, 42, 44, 46, 50, 54, and 58 MeV. The elastic scattering cross-sections were calculated using potential (14) with the parameter values from Table 1, which approximates the nucleus-nucleus potential ob-

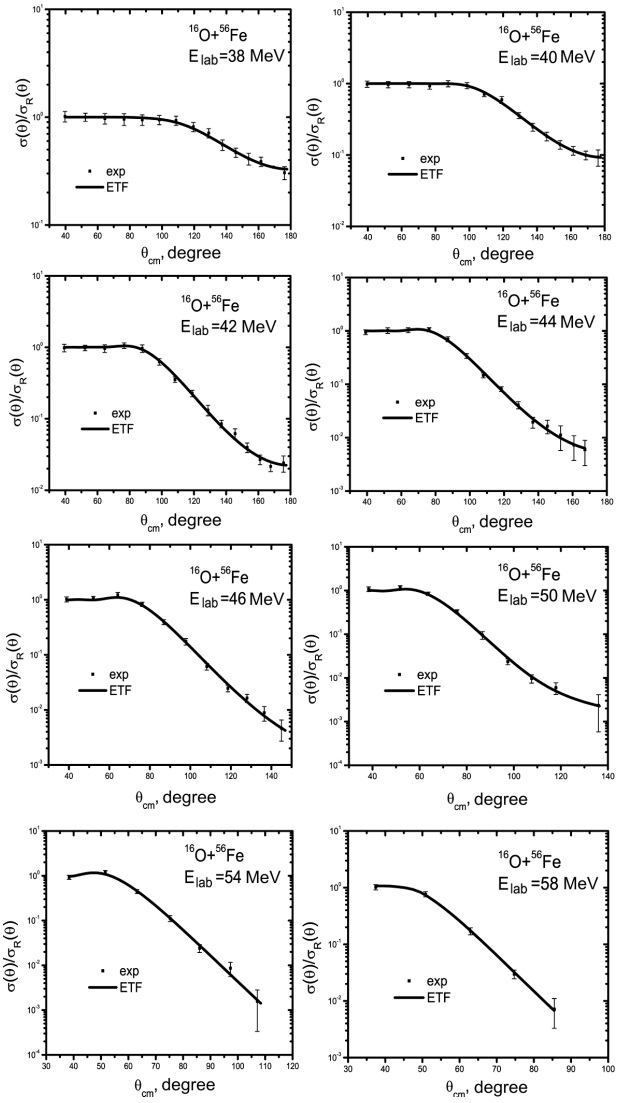

Fig. 5. Elastic scattering cross-sections for the ^{16}O + ^{56}Fe system at the beam energies $E_{\rm lab}$ = 38, 40, 42, 44, 46, 50, 54, and 58 MeV calculated in the modified Thomas–Fermi approximation with density-dependent Skyrme forces (ETF). Experimental data (exp) were taken from work [48]

tained in the framework of the modified Thomas–Fermi method. The parameters W_W, r_W, d_W, W_S, r_S, and d_S of the imaginary part were found by fitting the experimental elastic scattering cross-section values. The values of those parameters are presented in Table 2.

The results of calculations of the elastic scattering cross-sections for the ^{16}O+^{40}Ca, ^{16}O + ^{90}Zr, and ^{16}O + ^{56}Fe systems at the indicated beam energies $E_{\rm lab}$ are presented in Figs. 3, 4, and 5, respectively. In the figures, the data calculated for the elastic scattering cross-section were normalized to the Rutherford cross-section values. The experimental results were taken from works [45–48]. As one can see from the figures, the elastic scattering cross-sections calculated in this work are in a good agreement with the available experimental data.

5. Conclusions

In this work, in the framework of the modified Thomas–Fermi approach with density-dependent Skyrme forces, the nucleus-nucleus interaction potentials have been calculated for the systems ^{16}O + ^{40}Ca, ^{16}O + ^{56}Fe, and ^{16}O + ^{90}Zr, with the nucleon densities being obtained in the framework of the same approach. The SkM* parametrization [32] was used for Skyrme forces. The calculated potentials are found to contain a repulsive core, which is important for the calculations of elastic scattering cross-section. A successful analytic parametrization of the nucleus-nucleus interaction potential is found, which well describes the potential calculated in the framework of the modified Thomas–Fermi approach with density-dependent Skyrme forces.

On the basis of the obtained nucleus-nucleus interaction potentials, elastic scattering reactions are considered for the systems ^{16}O + ^{40}Ca, ^{16}O + ^{56}Fe, and ^{16}O + ^{90}Zr at various energies, and the corresponding elastic scattering cross-sections are calculated. Note that the same expression for the real part of the potential was used when carrying on calculations for each reaction at various energies, and only the imaginary part was fitted. It is shown that the found cross-sections are in a good agreement with the experimental data.

1. R. Bass. *Nuclear Reactions with Heavy Ion* (Springer, 1980) [ISBN: 978-3-642-05718-2].
2. G.R. Satchler. *Direct Nuclear Reactions* (Clarendon Press, 1983) [ISBN-13: 978-0198512691, ISBN-10: 0198512694].
3. P. Frobrich, R. Lipperheide. *Theory of Nuclear Reactions* (Clarendon Press, 1996) [ISBN: 9780198537830].
4. V.Yu. Denisov, V.A. Plujko. *Problems of Nuclear Physics and Physics of Nuclear Reactions* (Kyiv University Publ. Center, 2013) (in Russian).
5. J. Blocki, J.Randrup, W.J. Swiatecki, C.F.Tsang. Proximity forces. *Ann. Phys.* **105**, 427 (1977).

6. W.D. Myers, W.J. Swiatecki. Nucleus-nucleus proximity potential and superheavy nuclei. *Phys. Rev. C* **62**, 044610 (2000).
7. V.Yu. Denisov, V.A. Nesterov. Potential of interaction between nuclei and nucleon-density distribution in nuclei. *Phys. Atom. Nucl.* **69**, 1472 (2006).
8. V.Yu. Denisov. Interaction potential between heavy ions. *Phys. Lett. B* **526**, 315 (2002).
9. H.J. Krappe, J.R. Nix, A.J. Sierk. Unified nuclear potential for heavy-ion elastic scattering, fusion, fission, and ground-state masses and deformations. *Phys. Rev. C* **20**, 992 (1979).
10. V.Yu. Denisov, W. Norenberg. Entrance channel potentialsin the synthesis of the heaviest nuclei. *Eur. Phys. J. A* **15**, 375 (2002).
11. V.Yu. Denisov. Nucleus-nucleus potential with shell-correction contribution. *Phys. Rev. C* **91**, 024603 (2015).
12. A. Winther. Dissipation, polarization and fluctuation in grazing heavy-ion collisions and the boundary to the chaotic regime. *Nucl. Phys. A* **594**, 203 (1995).
13. V.Yu. Denisov, O.I. Davidovskaya. Repulsive core potential and elastic heavy-ion collisions. *Yad. Fiz.* **73**, 429 (2010).
14. V.Yu. Denisov, O.I. Davidovskaya. Repulsive core potential and elastic heavy-ion collisions. *Ukr. J. Phys.* **54**, 669 (2009).
15. K.A. Brueckner, J.R. Buchler, M.M. Kelly. New theoretical approach to nuclear heavy-ion scattering. *Phys. Rev. C* **173**, 944 (1968).
16. J. Fleckner, U. Mosel. Antisymmetrization effects in heavy ion potentials. *Nucl. Phys. A* **277**, 170 (1977).
17. O.I. Davidovskaya, V.Yu. Denisov, V.A. Nesterov. Nucleus-nucleus potential with repulsive core and elastic scattering. Part 1. Nucleus-nucleus interaction potential. *Yadern. Fiz. Energ.* **11**, No. 1, 25 (2010).
18. O.I. Davidovskaya, V.Yu. Denisov, V.A. Nesterov. Nucleus-nucleus potential with repulsive core and elastic scattering. Part 2. The elastic scattering cross sections with and without core. *Yadern. Fiz. Energ.* **11**, No. 1, 33 (2010).
19. V.Yu. Denisov, O.I. Davidovskaya. Elastic scattering of heavy ions and nucleus-nucleus potential with a repulsive core. *Bull. Russ. Acad. Sci. Phys.* **74**, 611 (2010).
20. O.I. Davidovskaya, V.Yu. Denisov, V.A. Nesterov. Effective nucleus-nucleus potential with the contribution of the kinetic energy of nucleons, and the cross-sections of elastic scattering and subbarrier fusion. *Ukr. J. Phys.* **62**, 473 (2017).
21. V.A. Nesterov. Effect of the Pauli Exclusion Principle and the Polarization of Nuclei on the Potential of Their Interaction for the Example of the ^{16}O+^{16}O System. *Phys. At. Nucl.* **76**, 577 (2013).
22. V.Yu. Denisov, O.I. Davidovskaya. Elastic ^{16}O+^{16}O scattering and nucleus-nucleus potential with a repulsive core. *Ukr. J. Phys.* **55**, 861 (2010).
23. O.I. Davydovska, V.Yu. Denisov, V.O. Nesterov. Nucleus-nucleus potential, the elastic scattering and subbarrier fusion cross sections for the system ^{40}Ca + ^{40}Ca. *Yadern. Fiz. Energ.* **19**, 203 (2018).
24. O.I. Davydovska, V.Yu. Denisov, V.A. Nesterov. Comparison of the nucleus-nucleus potential evaluated in the double-folding and energy density approximations and the cross-sections of elastic scattering and fusion of heavy ions. *Nucl. Phys. A* **989**, 214 (2019).
25. V.O. Nesterov, O.I. Davydovska, V.Yu. Denisov. Calculation of the cross-sections of sub-barrier fusion and elastic scattering of heavy ions using the modified Thomas–Fermi approach with the Skyrme force. *Yadern. Fiz. Energ.* **20**, No. 4, 349 (2019).
26. P. Ring, P. Schuck. *The Nuclear Many-Body Problem.* (Springer-Verlag, 1980) [ISBN: 978-3-540-21206-5].
27. M. Brack, C. Guet, H.B. Hakanson. Self-consistent semiclassical description of average nuclear properties – a link between microscopic and macroscopic models. *Phys. Rep.* **123**, 275 (1985).
28. M. Brack, R.K. Bhaduri, *Semiclassical Physics.* (Addison-Wesley Publ. Co, 1997) [ISBN-10: 0813340845; ISBN-13: 978-0813340845].
29. V.M. Strutinsky, A.G. Magner, V.Yu. Denisov. Density distributions in nuclei. *Z. Phys. A* **322**, 149 (1985).
30. J. Dobaczewski, W. Nazarewicz, P.G. Reinhard. Pairing interaction and self-consistent densities in neutron-rich nuclei. *Nucl. Phys. A* **693**, 361 (2001).
31. D. Vautherin, D.M. Brink. Hartree-Fock calculations with Skyrme's interaction. I. Spherical nuclei. *Phys. Rev. C* **5**, 626 (1972).
32. J. Bartel, P. Quentin, M. Brack, C. Guet, H.B. Hakansson. Towards a better parametrisation of Skyrme-like effective forces: A critical study of the SkM force. *Nucl. Phys. A* **386**, 79 (1982).
33. S.A. Fayans, S.V. Tolokonnikov, E.L. Trykov, D. Zawischac. Nuclear isotope shifts within the local energy-density functional approach. *Nucl. Phys. A* **676**, 49 (2000).
34. J.W. Negele. The mean-field theory of nuclear structure and dynamics. *Rev. Mod. Phys.* **54**, 913 (1982).
35. T.H.R. Skyrme. The effective nuclear potential. *Nucl. Phys.* **9**, 615 (1959).
36. H. Feshbach. The optical model and its justification. *Annu. Rev. Nucl. Sci.* **8**, 49 (1958).
37. H. Friedrich, L.F. Canto. Effective nucleus-nucleus potentials derived from the generator coordinate method. *Nucl. Phys. A* **291**, 249 (1977).
38. S. Hossain, M.N.A. Abdullah, Md. Zulfiker Rahman, A.K. Basak, F.B. Malik. Non-monotonic potentials for ^{6}Li elastic scattering at 88 MeV. *Phys. Scr.* **87**, 015201 (2013).
39. S. Hossain, Md. Masum Billah, M.M.B. Azad, F. Parvin. Non-monotonic potential description of alpha-Zr refractive elastic scattering. *Physica G* **40**, 105109 (2013).
40. S. Hossain, A.S.B. Tariq, A. Nilima, M. Sujan Islam, R. Majumder, M.A. Sayed, M.M. Billah, M.M.B. Azad, M.A. Uddin, I. Reichstein, F.B. Malik, A.K. Basak. Dependence of the ^{16}O+^{16}O nuclear potential on nuclear incompressibility. *Phys. Rev. C* **91**, 064613 (2015).
41. S. Misicu, H. Esbensen. Hindrance of heavy-ion fusion due to nuclear incompressibility. *Phys. Rev. Lett.* **96**, 112701 (2006).

42. S. Misicu, H. Esbensen. Signature of shallow potentials in deep sub-barrier fusion reactions. *Phys. Rev. C* **75**, 034606 (2007).
43. S. Misicu, F. Carstoiu. Absence of a maximum in the S factor at deep sub-barrier energies in the fusion reaction ^{40}Ca + ^{40}Ca. *Phys. Rev. C* **84**, 051601(R) (2011).
44. O.I. Davydovska, V.A. Nesterov, V.Yu. Denisov. The nucleus-nucleus potential within the extended Thomas–Fermi method and the cross-sections of subbarrier fusion and elastic scattering for the systems ^{16}O+^{58,60,62,64}Ni. *Nucl. Phys. A* **1002**, 121994 (2020).
45. J. Orloff, W.W. Daehnick. Elastic scattering of ^{16}O by ^{48}Ti, ^{40}Ca, ^{27}Al, ^{12}C, ^{7}Li, and ^{6}Li. *Phys. Rev. C* **3**, 430 (1971).
46. K.E. Rehm, W. Henning, J.R. Erskine, D.G. Kovar, M.H. Macfarlane, S.C. Pieper and M. Rhoades-Brown. Inelastic scattering of ^{16}O from ^{40,42,44,48}Ca. *Phys. Rev. C* **25**, 1915 (1982).
47. K.E. Rehm, J. Gehring, B. Glagola, W.C. Ma, W. Phillips, F.L.H. Wolfs. Energy dependence of one- and two-particle transfer reactions in the system ^{16}O+^{90}Zr. *Z. Phys. A* **A340**, 281 (1991).
48. A.W. Obst, D.L. McShan, R.H. Davis. Elastic scattering of ^{16}O by ^{56}Fe, ^{70,74}Ge, and ^{90}Zr. *Phys. Rev. C* **6**, 1814 (1972).

Received 14.11.22.
Translated from Ukrainian by O.I. Voitenko

В.О. Нестеров, О.І. Давидовська, В.Ю. Денисов

ПЕРЕРІЗИ ПРУЖНОГО РОЗСІЯННЯ, ОДЕРЖАНІ НА ОСНОВІ ПОТЕНЦІАЛУ МОДИФІКОВАНОГО МЕТОДУ ТОМАСА–ФЕРМІ З УРАХУВАННЯМ КОРА

Густини розподілу нуклонів та потенціали взаємодії між ядрами для реакцій ^{16}O + ^{40}Ca, ^{16}O + ^{56}Fe та ^{16}O + ^{90}Zr було розраховано в рамках модифікованого методу Томаса–Фермі, з урахуванням усіх доданків до членів другого порядку по $\hbar$ у квазикласичному розкладі кінетичної енергії. В якості нуклон-нуклонної взаємодії використовувалися сили Скірма, залежні від густини нуклонів. Знайдено параметризацію потенціалу взаємодії між ядрами, яка добре описує величину потенціалу, розрахованого у рамках модифікованого підходу Томаса–Фермі з залежними від густини силами Скірма. На основі одержаних потенціалів було обраховано перерізи пружного розсіяння, що добре узгоджуються з експериментальними даними.

Ключові слова: потенціал взаємодії між ядрами, модифікований метод Томаса–Фермі, розподіл густини нуклонів, поперечний переріз, кор відштовхування, пружне розсіяння.